COBEM 2021 26th International Congress of Mechanical Engineering
ABCM Associação Brasileira de Engenharia e Ciências Mecânicas
November 22-26, 2021, Virtual Congress, Brazil

COB-2021-1879
Fabrication and Characterization of Honeycomb Panels with Printed Circuit Board Faces

Pedro Alves
Mateus Sant'Ana
Tiago Rodrigues dos Santos
Manuel Nascimento Dias Barcelos Jr.
University of Brasilia, Setor Leste Projeção 1 Gama Leste – Brasilia DF
pedrohenriquedf11@gmail.com
mateus.s.santana.1@gmail.com
tiagorsantos97@gmail.com
manuelbarcelos@aerospace.unb.br

Abstract. *Sandwich Structures are made by two faces of a resistant material in its exterior. They have their core composed of a different material, usually with lower density and resistance than the material of the external faces. This paper proposed a manufacturing process of honeycomb sandwich panels made by Fused Deposition Modeling (FDM) – also known as 3D printing. In 3D printing, we employ some thermoplastic materials: polylactic acid (PLA), acrylonitrile butadiene styrene (ABS), and polyethylene terephthalate glycol (PETG). The faces are Phenolite laminate and Fiberglass laminate. To fabricate the sandwich panel, we used epoxy resin to bond the core to the faces. The Phenolite and Fiberglass laminates used for face sheets in honeycomb panels can still function as circuit boards. For instance, we can apply this configuration to optimize the volume of a small satellite. Therefore, this work aims to study honeycomb sandwich panel manufacturing with circuit boards for faces (Phenolite and Fiberglass laminates), and 3D printed thermoplastic cores (PLA, ABS, and PETG materials). We characterize the honeycomb sandwich specimens experimentally according to the standard ASTM C393 that regulates bending test and numerically by a finite element method simulation. The manufacture of the sandwich panels indicates good adhesion between the core and the faces. Comparing the bending tests' experimental and numerical results strictly in the elastic region presented satisfactory agreement.*

Keywords: *Honeycomb Structures, Sandwich Structures, Composite Materials, 3D printing, Printed Circuit Board*

1. INTRODUCTION

Sandwich structures are made by two faces of a resistant material in its exterior and have their core composed of a different material, usually with lower density and resistance than the material of the external faces (Gagliardo and Mascia, 2010). Honeycomb structures are widely used, especially in the aeronautics, aerospace industry. This is because of the mechanical properties that give them high mechanical strength, low specific mass, high energy absorption and good acoustic insulation (Bitzer, 1997). Sandwich panels also allow to decrease the cost of manufacturing parts by replacing the use of high performance materials with less noble materials (Carvalho, 2019), furthermore, according to Rezende (2000), it was possible to obtain a weight reduction between 20% and 30% and a cost reduction of 25% in the production of aerospace parts. There are recent researches dealing with the use of smart sandwich structures that can be applied to CubeSat, where Mughal *et al.* (2014) uses a sandwich structures with on board circuit in the faces.

Additive Manufacturing, popularly known as Rapid Prototyping or 3D Printing, is the manufacturing of parts and prototypes using computer-aided design (CAD). In conjunction with FDM (Fused Deposition Modelling), more complex models can be created more rapidly, reducing the steps needed to obtain a final product (Gibson *et al.*, 2015). Due to its ease of fabrication and reduced material costs, this new manufacturing method has been widely used in the aerospace, automotive, and biotechnology industries (Zou *et al.*, 2016).

Among the materials used in 3D Printing, PLA (Polylactic Acid), PETG (Polyethylene Glycol Terephthalate) and ABS (Acrylonitrile Butadiene Styrene) are the most prominent. PLA is one of the most widely used printing plastics because it is easier to print on compared to other thermoplastic materials such as PETG and ABS, in addition to being a biodegradable polymer. PETG is a modification of PET and is used in parts that need flexibility and durability (Santana *et al.*, 2018). ABS is a plastic used industrially in the production of toys, household items and decorative accessories, however, it is a plastic that is difficult to print as it needs thermal insulation to avoid warping (Ribeiro, 2019).

The printed circuit boards of electrical and electronic components have their base, also called laminate, made of thermoset materials such as phenolite, fiberglass and epoxy resin (also known as FR-4), composite or ceramic materials.

These laminates are covered by a thin layer of copper so that the circuit can be printed (Henrique Júnior *et al.*, 2013). Among the laminates mentioned, phenolite and fiberglass laminates stand out because they are easy to acquire in electronic component stores. Phenolite is a composite of special papers impregnated with phenolic resin that are laminated at high pressures and temperatures. Fiberglass and epoxy resin composite is a highly resistant composite, which makes it suitable for printed circuit board applications.

The objective of this work is to manufacture sandwich panels, with a core printed on thermoplastic material and using the faces of laminated materials used in printed circuit boards. This paper will also discuss the efficiency of sandwich panels built according to ASTM C393, comparing the relationship between displacement and force obtained in the bending test with the values obtained both analytically and by the finite element method.

2. METHODS

2.1 Honeycomb modeling

To conduct the study, destructive tests will be performed according to ASTM C393-00, in order to evaluate the mechanical properties of the sandwich panels manufactured. A bonding test will also be performed with the phenolite board and the printed materials, and also with the FR4 board and the printed materials. The lamination will be performed using epoxy resin.

The specimens were modeled with the aid of 3D modeling software. The core was modeled with an outer circle with a diameter of 5 mm, a wall thickness of 0.450 mm, and a height of 16 mm. Then repeat patterns were made in each cell of this core and a cut to the standard measurements of ASTM C393 which are 200 mm long by 75 mm wide. The Figure 1 shows the core made.

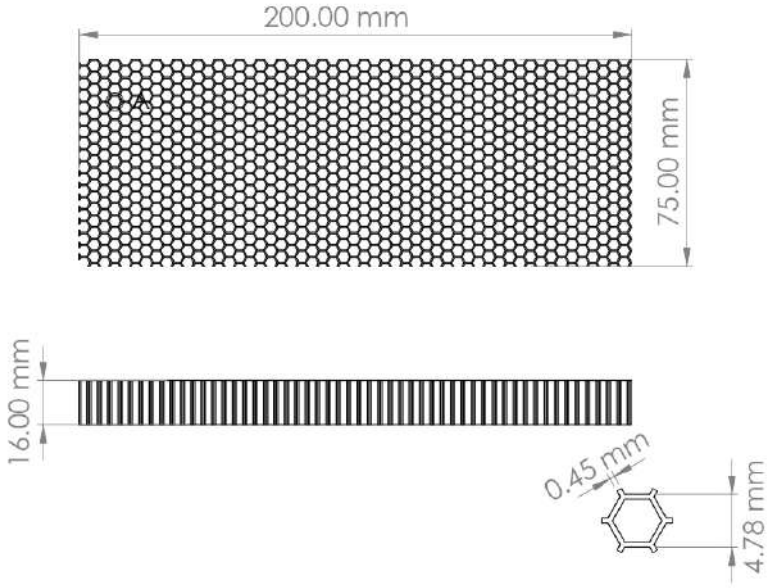

Figure 1. Honeycomb sandwich core

2.2 Analytical calculation

In order to obtain data to compare the values obtained both experimentally and numerically, a numerical analysis of the sandwich panel deflection was performed. For this, Eq. (1), defined by Bitzer (1997) was used.

$$\Delta = \frac{K_b P L^3}{D} + \frac{K_s P L}{h G_c b} \tag{1}$$

$$D = \frac{E_f t h^2 b}{2\lambda} \tag{2}$$

where Δ is the deflection of the beam, P is the applied load, L is the distance between the supports, D is the flexural modulus of rigidity of the panel, K_b is the bending deflection constant, K_s is the shear deflection constant and G_c is the shear modulus (or transverse modulus of elasticity) of the core. In Eq. (2), E_f is the face modulus of elasticity, h is the centroid distance, t is the face thickness, b is the width. To find the value of G_c, Eq. (3) can be used as a approach.

$$G_c = \frac{E_c}{2(1+\nu)} \tag{3}$$

where E_c is the Young's Modulus of the core material and ν its Poisson Ratio. And, to find and λ, Eq. (4) is used.

$$\lambda = 1 - \nu^2 \tag{4}$$

Analytical calculations were performed using a constant K_b equal to 0.002604, a K_s equal to 0.125, and a face thickness t with a value of 1.6 mm. The analytical calculations and the numerical modeling of bending were carried considering a variable applied load and a length span of 150 mm.

To find the shear stress in the core in the faces and the normal stress, Eq. 5 and Eq. 6 were used.

$$F_s = \frac{P_{max}}{(d+c)b} \tag{5}$$

$$\sigma_f = \frac{P_{max} L}{2t(d+c)b} \tag{6}$$

where F_s is the core shear stress, P_{max} is the maximum force before the failure, d is the sandwich thickness, c is the core thickness and σ_f is the facing stress.

2.3 Numerical analysis

The structural simulation was performed in commercial software based on the Finite Element Method (FEM). Initially, the mechanical properties of the materials used were set. The materials of the core and the faces were modeled as isotropic, following what was studied by Wernke (2019). The properties are shown in Table 1.

Table 1. Properties of the materials used for the analytical calculation

Material	Modulus of Elasticity [MPa]	Poisson Ratio
FR-4(1)	3.42	0.25
ABS(2)	2.2	0.38
PETG(3)	1.5	0.4
PLA(4)	2.85	0.3

(1) Properties obtained according to Madhukar *et al.* (2018)

(2) Properties obtained according to Santos *et al.* (2020)

(3) Properties obtained according to Santana *et al.* (2018)

(4) Properties obtained according to Sant'Ana *et al.* (2021)

The geometry used was the same as that modeled for printing, however, the faces were also added to the 3D design. The model was then exported to the simulation software in .step format to avoid inconsistencies in the geometry. Next, splits were made on the top and bottom faces. The first split was made in the middle of the top face, so as to divide it into two equal parts. The second split, as well as the third split, was made 25 mm from the corners, so that the distance between the two splits was 150 mm.

Next, the geometry mesh was created using a 2 mm tetrahedral element. The boundary conditions used in the simulation are the same as those defined by the 3-point bending test. A fixed support was defined on the lines that are 25 mm from the end and a load was applied on the line dividing the top face. Figure 2 shows how boundary conditions were set. From this simulation it was expected to obtain the value of the displacement in the direction of the applied force.

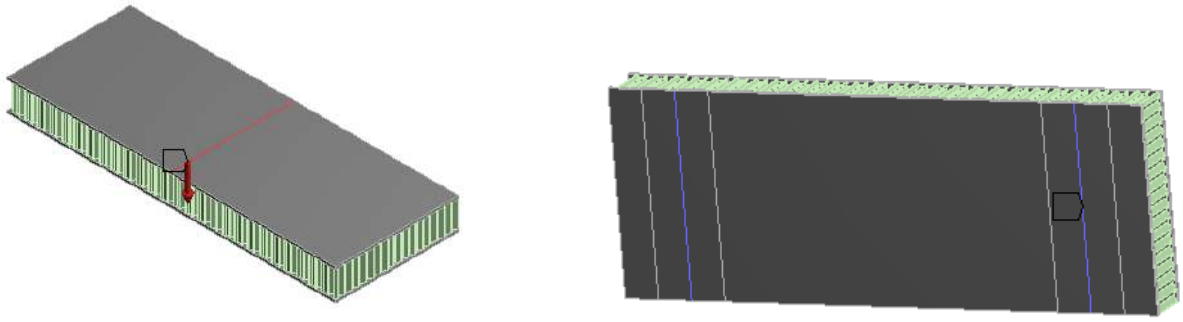

(a) Applied Force (b) Fixed Support

Figure 2. Boundary Conditions

2.4 Manufacturing process

The cores were fabricated using a 3D FDM printer with a printing area of 300 mm length, 300 mm width, and 300 mm height, with the printing parameters, extruder nozzle temperature at 200 °C, table temperature at 60 °C with a material deposition speed per layer of 80 mm/s, nozzle diameter of 0.4 mm, layer height of 0.200 mm, and 100% fill. The filament used for making the specimens was natural PLA from the manufacturer 3DLab supplier.

To produce the specimen, adhesion tests were performed between the materials and the epoxy resin. The epoxy resin used will be Epoxy Resin 2004 and Epoxy Hardener 3154. The adhesion test was carried out with the variations Phenolite and ABS, Phenolite and PETG, Phenolite and PLA, Fiberglass and ABS, Fiberglass and PETG, Fiberglass and PLA.

To perform the adhesion test, cores were printed using ABS, PETG, and PLA. The laminate faces were purchased with a dimension of 200 mm long, 150 mm wide and 1.6 mm thick. Then the faces and cores were cut using a micro grinder. It is possible to see the cores in Figure 3 (a). To improve adhesion, the laminate faces were sanded to remove the protective film. Figure 3 (b) shows the faces after the sanding process.

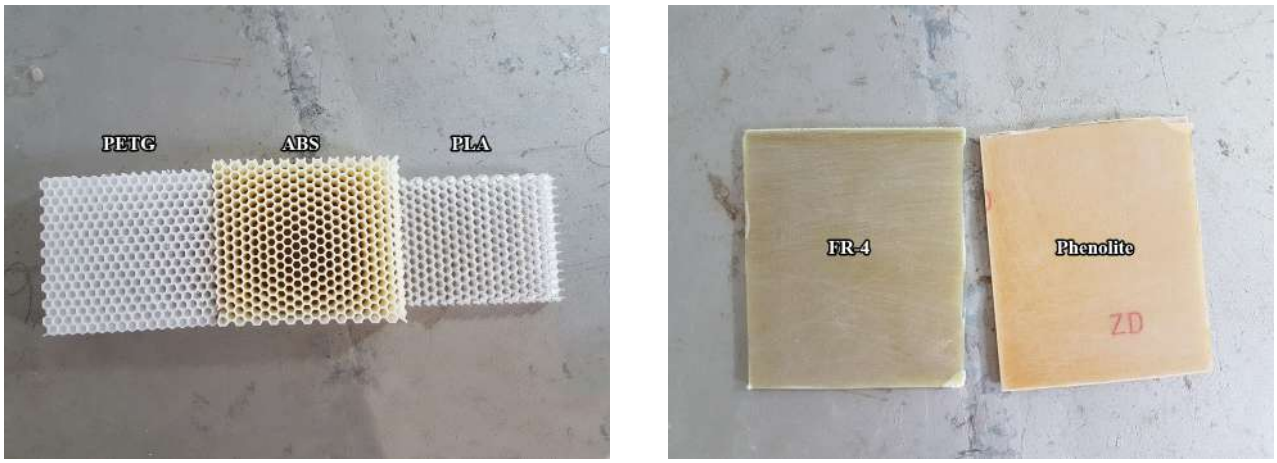

(a) Cores used in bonding test (b) Laminate faces sanded

Figure 3. Materials used in adhesion test

The next step was to prepare the epoxy resin according to the supplier's specifications. A ratio of 100% epoxy resin to 50% catalyst was used. Next, the cores and faces went through a lamination process. This process consists of fixing the core and faces using the epoxy resin. The resin was spread on the faces and then they were positioned on the workbench.

To perform the lamination, the specimens were subjected to vacuum. According to Sant'Ana and Carvalho (2020), the use of vacuum reduces bubbles and voids in the resin, improving the adhesion between the materials.

The laminating table was set up as follows, initially an outline was made using Tacky Tape to perform the sealing, then a layer of wax was applied to prevent the specimens from sticking to the table. Next, the specimens were positioned, and above them a layer of Peel Ply, a layer of perforated film, and a layer of breather. A hose connected to a vacuum pump was inserted and the system was covered with a vacuum bag (Sant'Ana *et al.*, 2019). The bodies remained under vacuum for a period of six hours. Figure 4 demonstrates how the system was assembled and Fig. 6 shows the manufactured specimen.

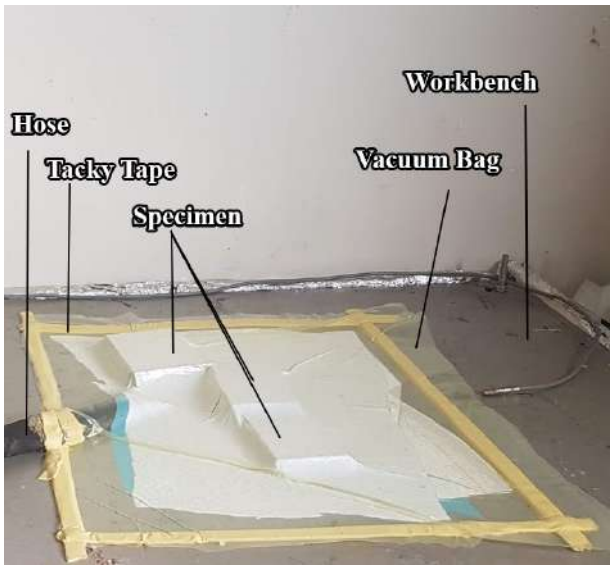

Figure 4. Lamination bench

2.5 Three Points Bending Test - ASTM C393

To analyze the strength of the manufactured sandwich panels, a test according to ASTM C393 standards will be performed. Five specimens in the combination PLA and FR4 were submitted to the destructive 3-point test. Then, with the data obtained, it will be possible to make a comparison between the analytical calculation and the numerical analysis performed. Figures 5 (a) and (b) illustrates how the test will be performed.

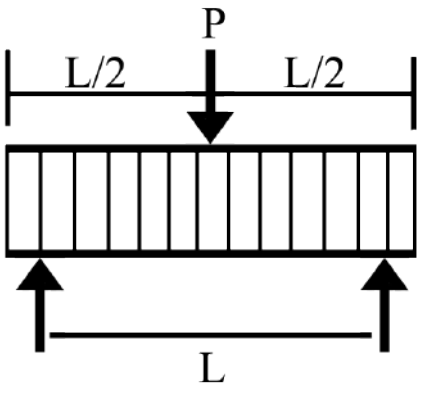

(a) Illustrated (Adapted from ASTM C393)

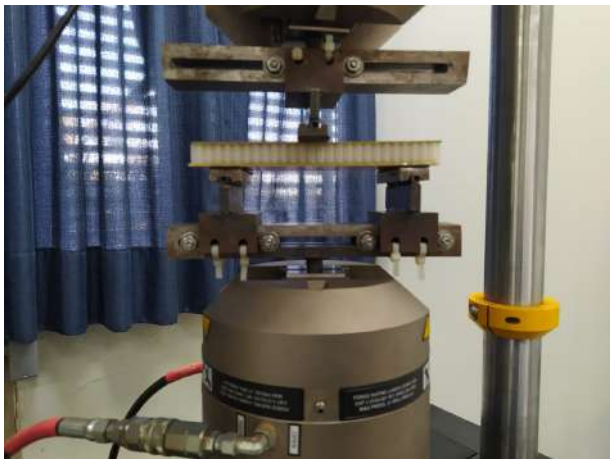

(b) Performed test

Figure 5. Three Points Bending test

The test was performed using Instron 8801 servohydraulic fatigue testing system, the speed of the test was set to 1 millimeter per minute, so that failure could occur between 3 minutes and 6 minutes. The length span L between the supports was set as 150 millimeters and the load, as defined by ASTM 393.

3. RESULTS

After the adhesion test, a good adhesion was noticed between the PLA-FR4, PLA-Phenolite, PETG-FR4 and PETG-Phenolite combinations, however, the ABS core did not adhere to the phenolite faces. In addition, the material presented printing problems, such as warping, so ABS cores were not produced.

The specimens in the PLA-FR4 combination had a mass of 199.43 $\pm$ 5.80 g and a density of 0.692 $\pm$ 0.020 g/cm^3. The PETG-FR4 combination specimens had a mass of 190.70 $\pm$ 7.59 g and a density of 0.662 $\pm$ 0.026 g/cm^3. Figure 6 shows a PLA-FR4 specimen manufactured.

Figure 6. PLA-FR4 Specimen

In order to compare the displacement values obtained by the analytical and numerical method, a force of 1000 N was chosen. The results obtained are shown in the Table 2 and indicate a good correlation between the analytical and numerical data. The simulated geometry can be seen in Figure 7.

Figure 7. Simulated geometry displacement contour

Table 2. Results of deflection obtained by analytical calculation, numerical modeling and experimental tests

Specimen material	**Analytical displacement [mm]**	**Numerical displacement [mm]**	**Experimental displacement [mm]**
FR-4 and ABS	1.0974	0.9814	-
FR-4 and PETG	1.1148	1.1432	1.0547
FR-4 and PLA	1.0876	0.8886	1.0008

From Table 2 above, it is possible to determine the percentage error between each of the methods in relation to the experimental value obtained. The percent error is shown in Table 3.

Table 3. Percent error in relation to the experimental value obtained

	PETG-FR4	**PLA-FR4**
Analytical	5.70%	8.67%
Numerical	8.39%	11.21%

After performing the tests, it was possible to obtain the maximum load value of 8086.6 N and a maximum displacement of 6.1481 for the specimens. It was also possible to compare the displacement between the analytical, numerical and experimental data for the PLA-FR4 combination in Figure 8(a). For the PETG - FR4 combination, the maximum load was 3635.5 N and the maximum displacement was 3.7420 mm. It is possible to compare the displacement between analytical, numerical and experimental data in Figure 8(b).

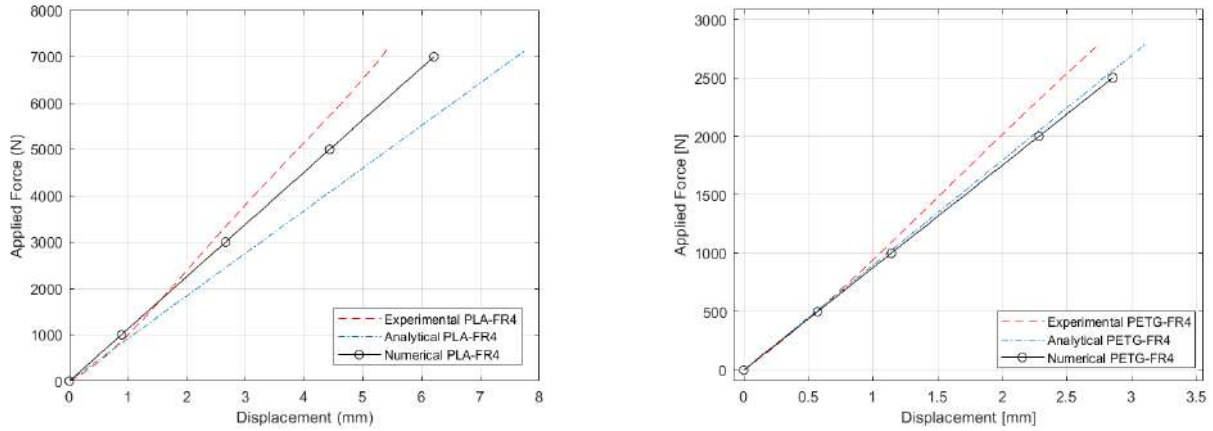

(a) PLA-FR4 (b) PETG-FR4

Figure 8. Comparison of experimental, numerical and analytical displacements

In Figure 9 it is possible to compare the force and displacement curves of the PLA-FR4 and PETG-FR4 combinations. It can be seen that the PLA-FR4 combination withstood higher loading, resulting in a larger displacement, this is due to the ultimate stress of PETG being lower than the ultimate stress of PLA. It is also noticeable that for loads below 1000 N the curves are very close, this is due to the material of the faces of both panels being the same.

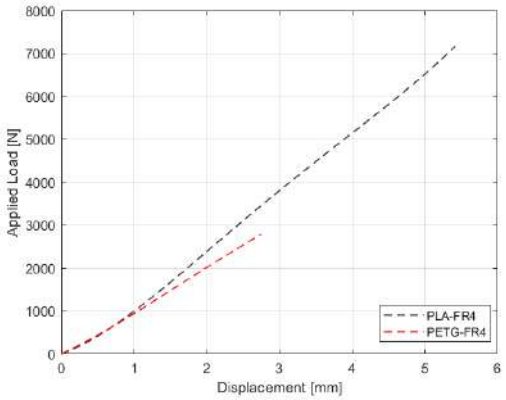

Figure 9. Comparison of PLA-FR4 and PETG-FR4

Therefore, one can compare the strength, displacement, normal stress on the faces, shear stress on the core, and density between the PLA-FR4 and PETG-FR4 combinations. After doing the percentage difference, an increase of more than 100% in the maximum load and maximum stresses was noticed, while the change in density was only 4.53%. Table 4 shows the comparison of the properties of PLA-FR4 and PETG-FR4 and Figure 10 shows the comparison of the stresses.

Table 4. Comparison of the properties of PLA-FR4 and PETG-FR4

Materials	**Maximum Force [N]**	**Maximum Displacement [mm]**	**Facing Stress [MPa]**	**Core Shear Stress [MPa]**	**Density [g/cm^3]**
PLA-FR4	8086.6	6.1481	143.58	3.06	0.692
PETG-FR4	3635.5	3.7420	64.55	1.38	0.662
Percent difference	122.43%	64.30%	122.43%	121.74%	4.53%

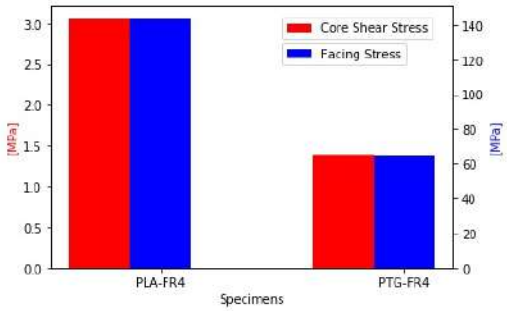

Figure 10. Comparison of stresses obtained

In addition, failure modes of honeycomb panels provide important aspects. For both PLA-FR4 and PETG-FR4 tested specimens, it was possible to notice a core fracture, described by Bitzer (1997) as Transverse Shear Failure, it is ilustrated in Figure 11 (a). This type occurs due insufficient core shear strength. Figure 11 (b) shows the fracture of the sandwich panels.

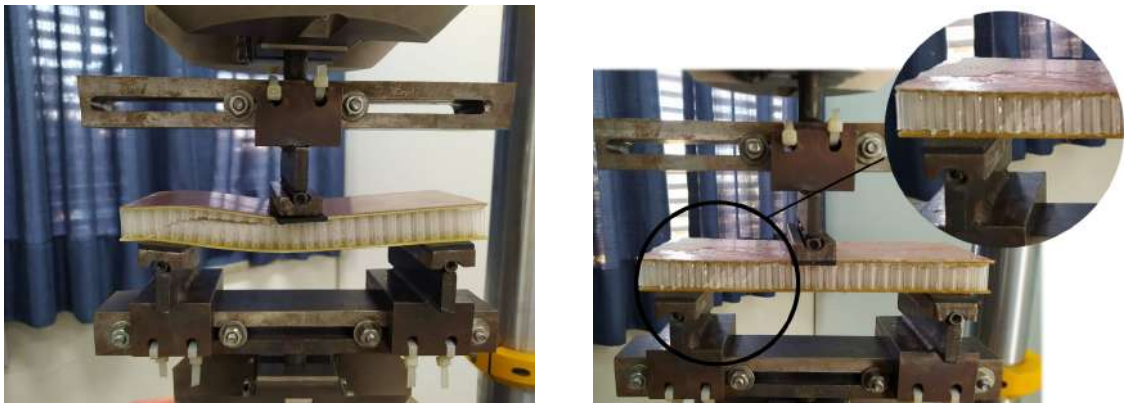

(a) PLA-FR4 fracture. (b) PETG-FR4 Fracture

Figure 11. Specimens Failure

According Petras (1998) it is possible to predict failure modes as well as analyze failure mode agents. For this study there were no failures arising from the manufacturing process, such as the face delamination observed by Carvalho (2019) in they aluminum specimens. All the failures presented brittle behavior, i.e. they did not demonstrate a strain hardening zone. This fragile behavior was expected, as described in studies conducted by Ribeiro (2019) and Santana *et al.* (2018).

4. CONCLUSION

The results obtained by the analytical calculation show that the face material has more influence on the deflection than the core materials, and showed a small deflection compared to the applied load, making it feasible to study these materials in CubeSats. The manufacture of the sandwich panels indicates good adhesion between the core and the faces. Comparing the bending tests' analytical and numerical results strictly in the elastic region presented satisfactory agreement. It was also possible to see that simplifying the core shear modulus G_c as the load shear modulus gives satisfactory results for small loads.

5. ACKNOWLEDGEMENTS

We thank Professor Manuel Nascimento Dias Barcelos Júnior for purchasing the materials and for the technical support during the project.

6. REFERENCES

ASTM, 2000. "Standard Test Method for Flexural Properties of Sandwich Constructions". ASTM International.

Bitzer, T., 1997. *Honeycomb Technology - Materials, design, manufacturing, applications and testing*. Springer-Science + Business Media, B.V.

Carvalho, L.R., 2019. "Fabricação e caracterização de estruturas sanduíche tipo colmeia com núcleo impresso por fusão e deposição de material termoplástico". Term Paper, UnB (Universidade de Brasília), Brasília, Brazil.

Gagliardo, D.P. and Mascia, N.T., 2010. "Análise de estruturas sanduíche: parâmetros de projeto". *Ambiente Construido*, Vol. 10, pp. 247–258.

Gibson, I., Rosen, D. and Stucker, B., 2015. *Additive Manufacturing Technologies - 3D Printing, Rapid Prototyping, and Direct Digital Manufacturing*. Springer.

Henrique Júnior, S.S., Moura, F.P., Correa, R.S., Afonso, J.C., Vianna, C.A. and Mantovano, J.L., 2013. "Processamento de placas de circuito impresso de equipamentos eletroeletrônicos de pequeno porte". *Química Nova*, Vol. 36, pp. 570–576.

Madhukar, D.K., Dutta, S.R., Mahto, P.K., Sinha, A.K. and Das, P.P., 2018. "Random spectral analysis of integrated avionics module". *IOP Conference Series: Materials Science and Engineering*, Vol. 377.

Mughal, M.R., Ali, A., Ali, H. and Reyneri, L.M., 2014. "Smart honeycomb tile for small satellites". In *IEEE Aerospace Conference Proceedings 2014*. Big Sky, USA.

Petras, A., 1998. *Design od Sandwich Structures*. Ph.D. thesis, Cambridge University, Engineering Department.

Rezende, M.C., 2000. "O uso de compósitos estruturais na indústria aeroespacial". *Ambiente Construido*, Vol. 10, pp. E4–E10.

Ribeiro, G.P., 2019. "Caracterização Mecânica de Estruturas Manufaturadas por Adição de Material Termoplástico com diferentes níveis e formas de preenchimento". Term Paper, UnB (Universidade de Brasília), Brasília, Brazil.

Santana, L., Alves, J.L., Netto, A.C.S. and Merlini, C., 2018. "Estudo comparativo entre PETG e PLA para impressão 3D através de caracterização térmica, química e mecânica". *Revista Matéria*, Vol. 23.

Sant'Ana, M.S., Alves, P.H.S., Santos, T.R. and Jr., M.N.D.B., 2021. "Análise numérica e experimental de painéis sanduíche fabricados com núcleo termoplástico e faces laminadas". In *COBEF - Congresso Brasileiro de Engenharia de Fabricação*. Curitiba, Brazil.

Sant'Ana, M.S. and Carvalho, L.R., 2020. "Thermoplastic-composite honeycomb panels manufacturing process for application in cubesat". In *IAA*. São José dos Campos, Brazil.

Sant'Ana, M.S., Gomes, M.L.C. and Jr, M.N.D.B., 2019. "Analysis of the influence of the cure and post-cure processes on fiberglass composites". In *COBEM*. Curitiba, Brazil.

Santos, T.R., Pastrana, M.A., Britto, W., Muñoz, D.M. and Jr., M.N.D.B., 2020. "The effects of printing parameters on mechanical properties of a rapidly manufactures mechanical ventilator". In *CBEB*. Vitória, Brazil.

Wernke, A.P., 2019. "Caracterização e avaliação da preditibilidade de modelos isotrópicos e ortotrópicos para materiais impressos com foco em otimizações topológicas". Term Paper, UnB (Universidade de Brasília), Brasília, Brazil.

Zou, R., Xia, Y., Liu, S., Hu, P., Hou, W., Hu, Q. and Shan, C., 2016. "Isotropic and anisotropic elasticity and yielding of 3d printed material". *Composites Part B*, Vol. 99, pp. 506–513.

7. RESPONSIBILITY NOTICE

The authors are solely responsible for the printed material included in this paper.